Supplementary Information

Supplementary Fig. 1. Howler monkeys identified at the PEAL, São Paulo municipality, during the YFV epizootic outbreak at different decomposition stages. (**a**) and (**b**) early decomposition stage (0–2 days PM), (**c**) medium decomposition stage (3–5 days PM), (**d**) and (**e**) advanced decomposition stages (>5 days PM). PM=post-mortem.

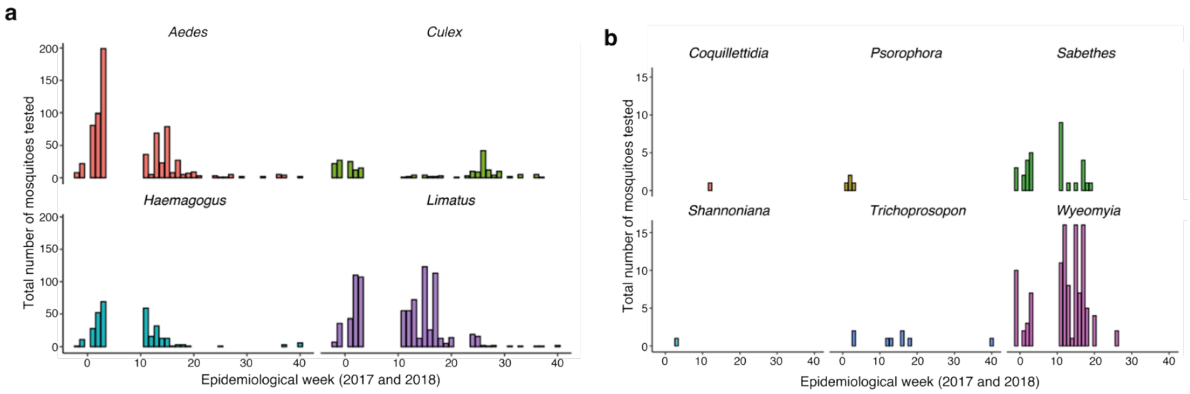

Supplementary Fig. 2. More abundant (a) and less abundant (b) mosquito genera collected at PEAL. Total number of mosquitoes tested (number of mosquitoes multiplied by pool size) per epidemiological week.

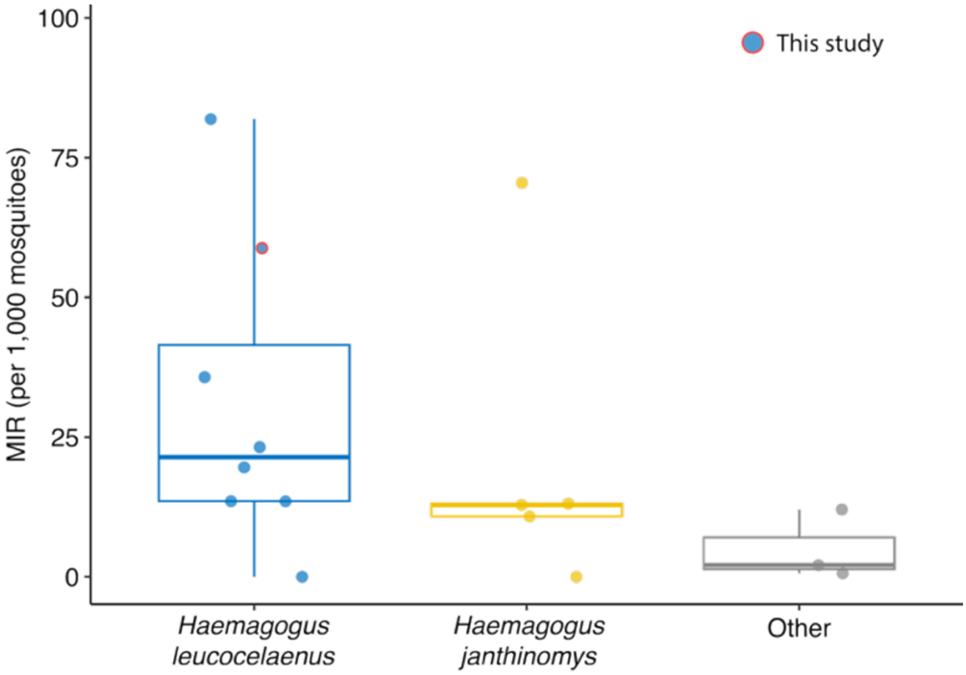

Supplementary Fig. 3. Minimum infection rates (MIR) for primary YFV vectors in Brazil. Data was compiled from studies conducted across four Brazilian States (Espirito Santo, Maranhao, Minas Gerais and Rio de Janeiro) for species-specific MIRs[1–3]. Only studies that tested 10 or more pools per specie are included. The MIR for *Hg. leucocelaenus* estimated in our study is shown in a blue circle with a red stroke. To contextualise our data, we also compared RT-PCR Ct from *Hg. leucocelaenus* obtained in PEAL (n=9) with reported Cts reported in other studies[1,4,5] from *Hg. leucocelaenus* (n = 64), *Hg. janthinomys/ Hg. janthinomys-capricornii* (n = 25) and "Other" species (n = 29, includes *Psorophora ferox, Sabethes albiprivus, Sa. chloropterus, Sa. identicus, Sa. purpureus, Aedes serratus, Ae. scapularis, Ae. albopictus, Ae. taeniorhynchus*).

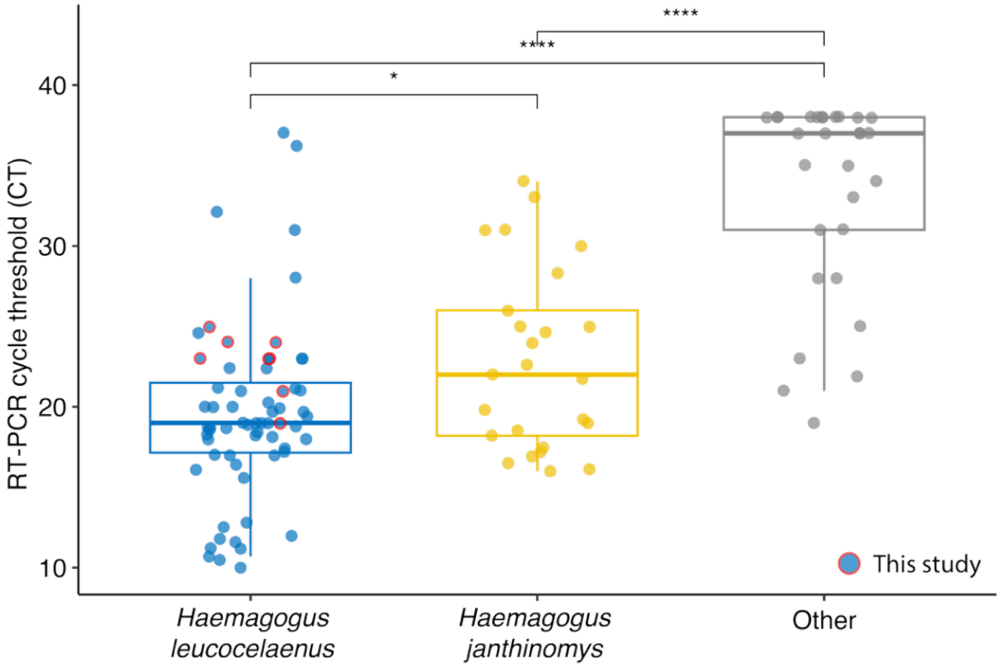

Supplementary Fig. 4. Distribution of YFV RT-PCR cycle thresholds values obtained from mosquito pools from this and other studies[1,4,5]. Pools were grouped in three categories: *Haemagogus leucocelaenus* (median Ct = 19.5; blue circles, *n* = 64), *Ha. janthinomys* (median Ct = 22.9; yellow circles, *n* = 25, also includes *Ha. janthinomys/capricornii*) and "Other" (median Ct = 33.4; grey, *n* = 29) comprising *Psorophora ferox*, *Sabethes albiprivus*, *Sa. chloropterus*, *Sa. identicus*, *Sa. purpureus*, *Aedes serratus*, *Ae. scapularis*, *Ae. albopictus* and *Ae. taeniorhynchus*. Boxes represent the inter-quartile range and horizontal lines denote the median. Pools generated in the present study are outlined in red. Pairwise comparisons were performed with two-sided Wilcoxon rank-sum tests: *Hg. leucocelaenus* vs *Hg. janthinomys*, *P* = 0.044*; Hg. leucocelaenus vs Other, P = 0.0008* and *Hg. janthinomys* vs Other, *P* < 0.0001. Asterisks above brackets denote significance levels (**P* < 0.05, *****P* < 0.001).

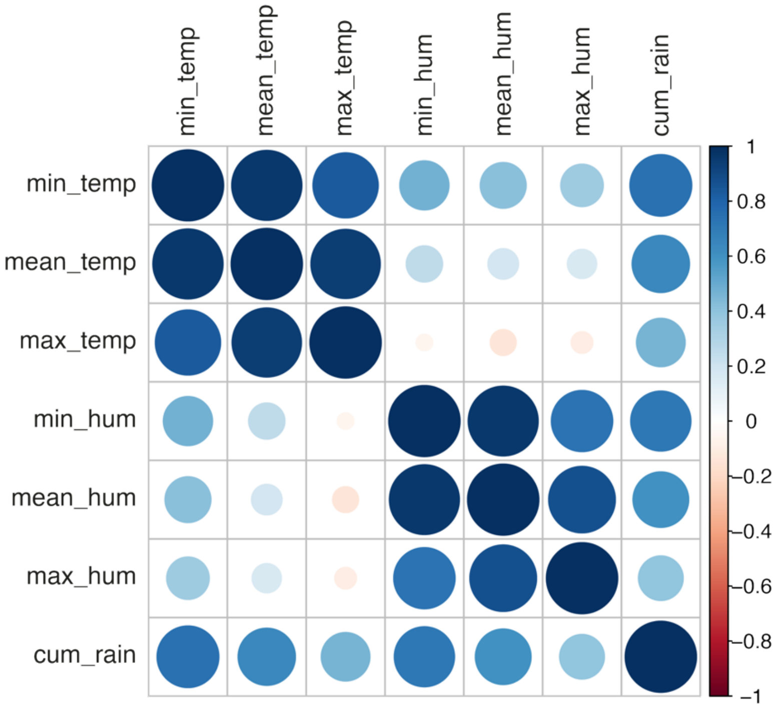

Supplementary Fig. 5. Pairwise correlations among monthly meteorological covariates used in the *Hg. leucocelanus* models. Pearson correlation coefficients between seven z-standardised climate variables (minimum, mean and maximum temperature; minimum, mean and maximum relative humidity; and cumulative rainfall) are shown as coloured circles. Circle area and colour intensity scale with correlation magnitude as shown on the right, with blue denoting positive and red denoting negative associations.

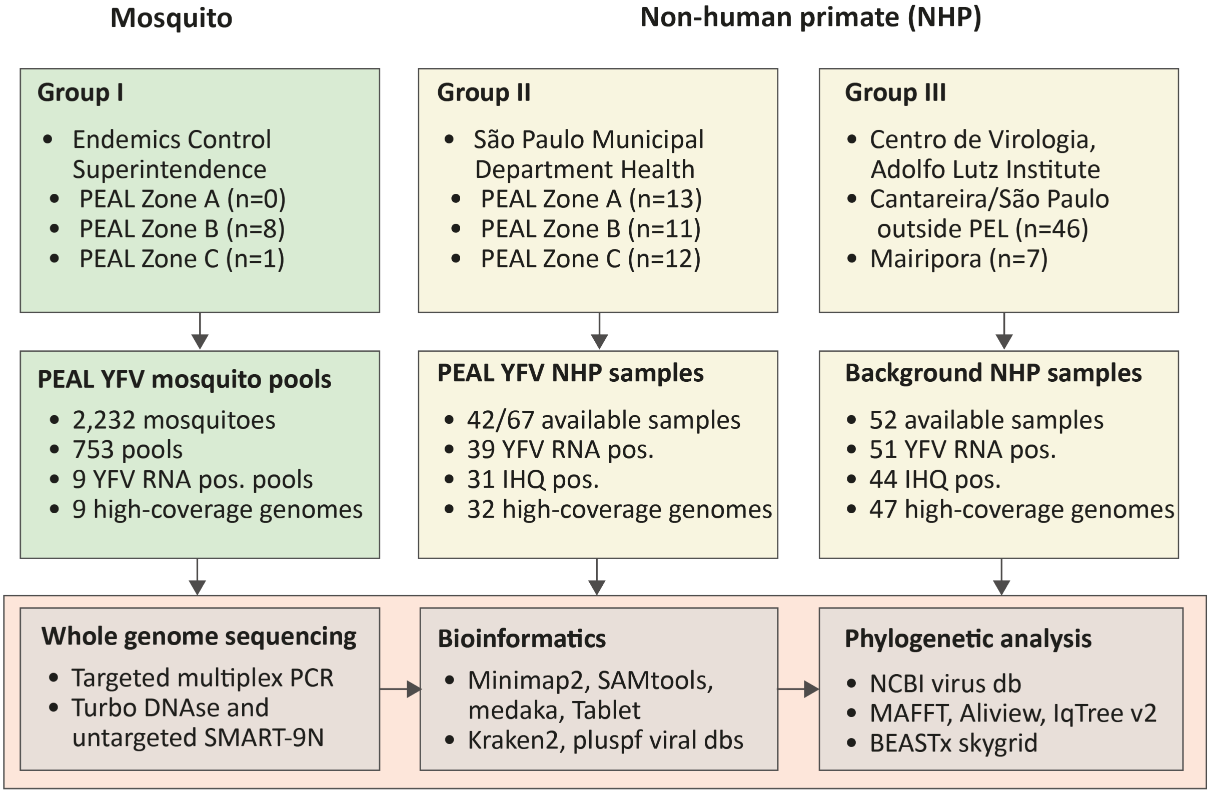

Supplementary Fig. 6. Flowchart of the sample collection, testing and sequencing across Groups I, II and III (GI–GIII). NHP=Nonhuman primate. MO=mosquito vector.

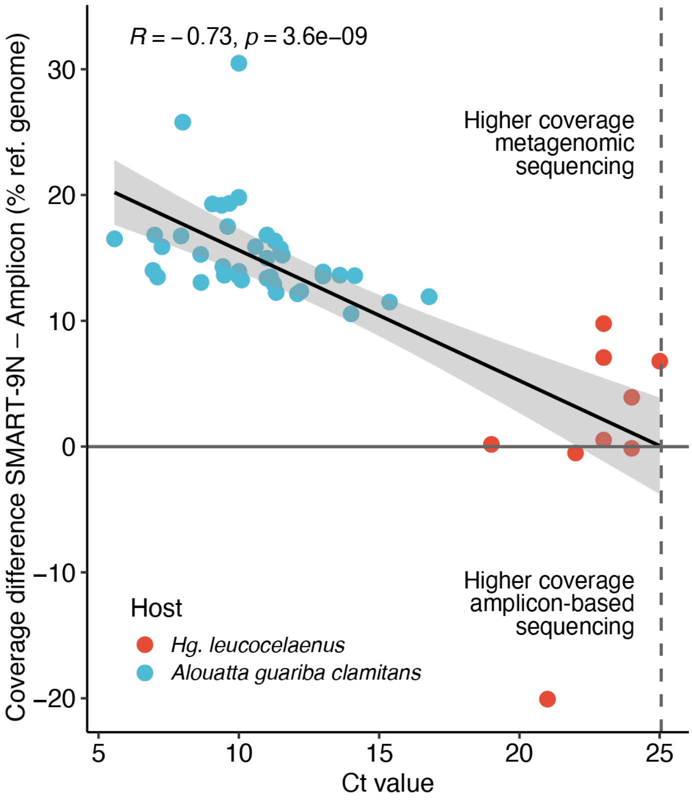

Supplementary Fig. 7. Relationship between RT-PCR cycle threshold (Ct) values and difference between consensus sequence coverage for paired samples sequenced with metagenomic and multiplex PCR (amplicon-based) nanopore sequencing. Dots represent paired sequenced samples (blue = nonhuman primates, red = mosquitoes). Solid black line shows linear regression line across 49 samples (shaded band = 95 % CI; *n* = 49). Pearson's ρ and *p*-value are inset. The horizontal grey line denotes zero difference (that is, identical coverage for both methods), and the vertical dashed line marks the Ct at which the fitted regression predicts no difference (Ct ≈ 25). Sample sizes: primates *n* = 40, mosquitoes *n* = 9. Pearson's ρ= -0.73, $p < 0.0001$.

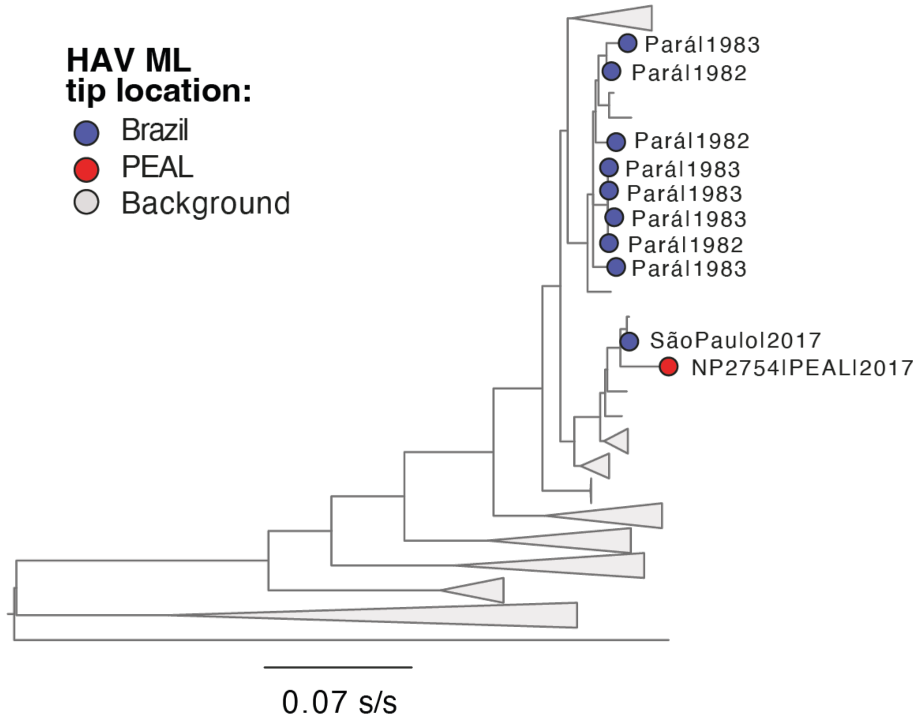

Supplementary Fig. 8. Maximum likelihood phylogeny of Hepatitis A virus complete genome sequences. Red tup obtained from an *A. guariba* individual at PEAL (NP2754). Tip colours denote sampling location: blue = Brazilian genomes; red = PEAL NP2754 isolate; open = global background. The 2017 PEAL genome nests within the Brazilian clade that includes a contemporary 2017 São Paulo strain. Nodes outside of Brazil are either filled triangles or collapsed. Branch lengths are proportional to nucleotide substitutions per site. The geographic location for PEAL NP2754 is shown in **Fig. 1** (main text).

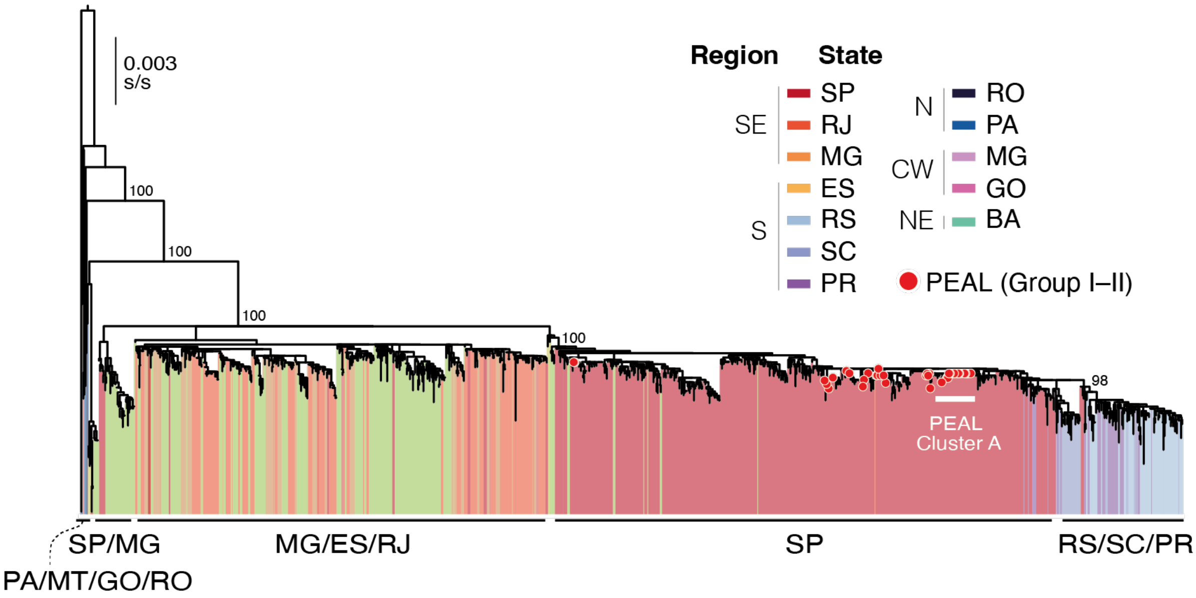

Supplementary Fig. 9. Maximum likelihood phylogeny of YFV genomes from Brazil. The tree was inferred from the YFV "Brazil dataset" (n=1,063). Terminal branches are coloured by the Brazilian state of sampling and grouped by macro-region (SE=Southeast, S=South, CW=Centre-West, N=North, NE=Northeast). State abbreviations are as follows: PA=Pará, MT=Mato Grosso, GO=Goiás, RO=Rondônia, SP=São Paulo, MG=Minas Gerais, ES=Espírito Santo, RJ=Rio de Janeiro, RS=Rio Grande do Sul, SC=Santa Catarina, PR=Paraná. Red circles highlight YFV genomes generated from nonhuman primates and mosquito pools at PEAL (groups I and II). The main lineage containing these sequences is labelled PEAL Cluster A. Numerical values on internal nodes indicate bootstrap support (%).

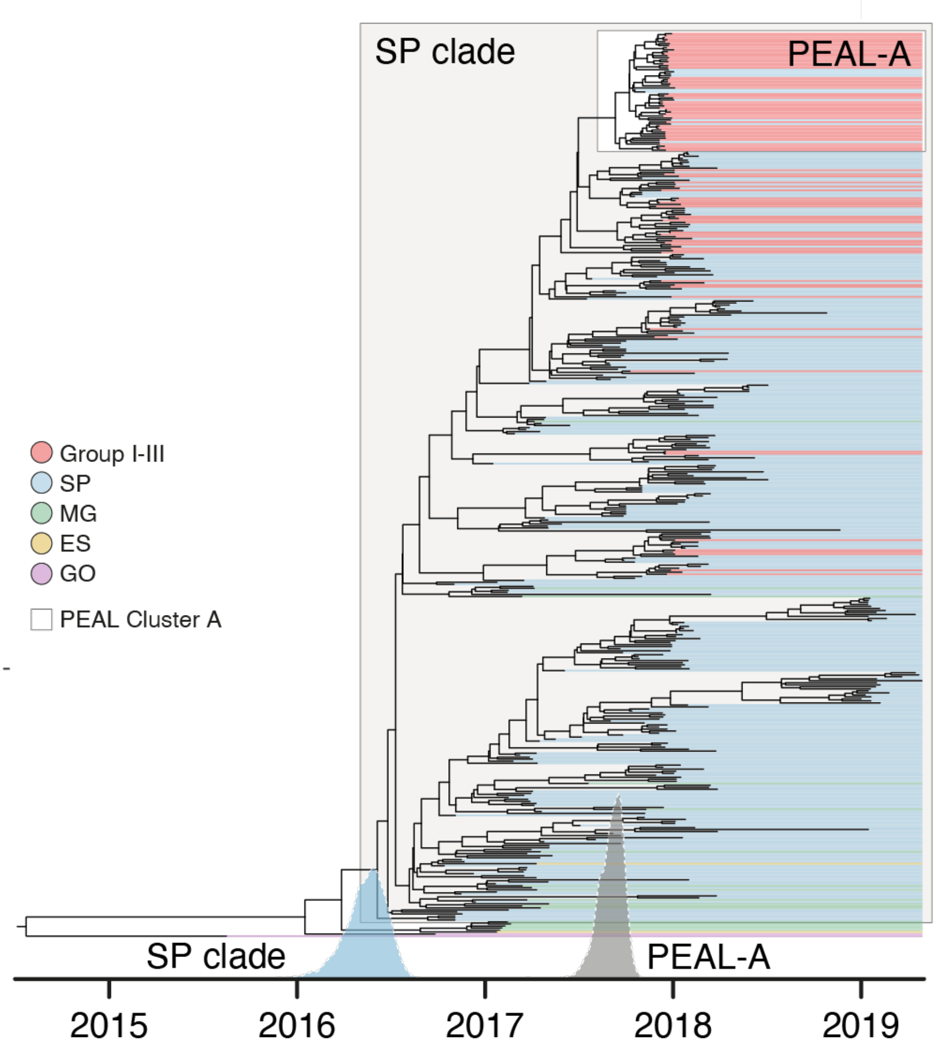

Supplementary Fig. 10. Time-scaled phylogeny of the São Paulo dataset. The Bayesian maximum-clade-credibility tree was reconstructed from 450 YFV genomes sampled predominantly in southeastern Brazil. The x-axis is in calendar years. Terminal branches are coloured according to Brazilian state of sampling (PEAL Group I-II and background sequences are show in red). Grey shaded rectangle delineates the monophyletic YFV_{SP} clade reported previously[6]; white box highlights PEAL Cluster A (PEAL-A) within that clade. KDE curves give posterior distribution of the TMRCA for SP clade, and PEAL-clade estimated using this dataset.

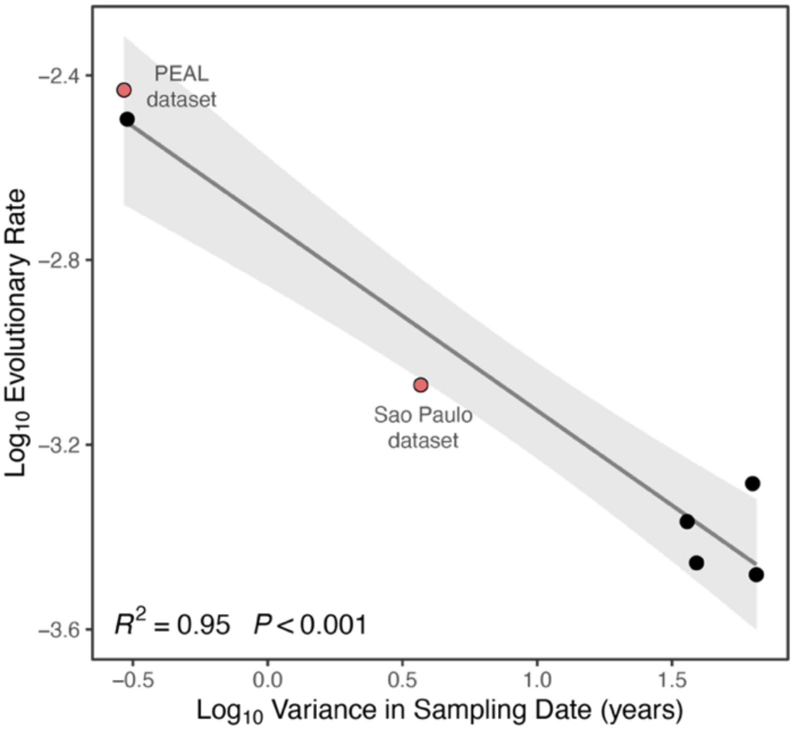

Supplementary Fig. 11. Time-dependency of YFV South American genotype 1 evolutionary rates. Median evolutionary rates obtained for the PEAL and São Paulo datasets are shown in red circles. Estimates from other previously published YFV datasets[7–11] are shown in black circles. Variance in sampling dates ranged between 107 days (PEAL dataset), 3.7 years (São Paulo dataset) to 65 years.

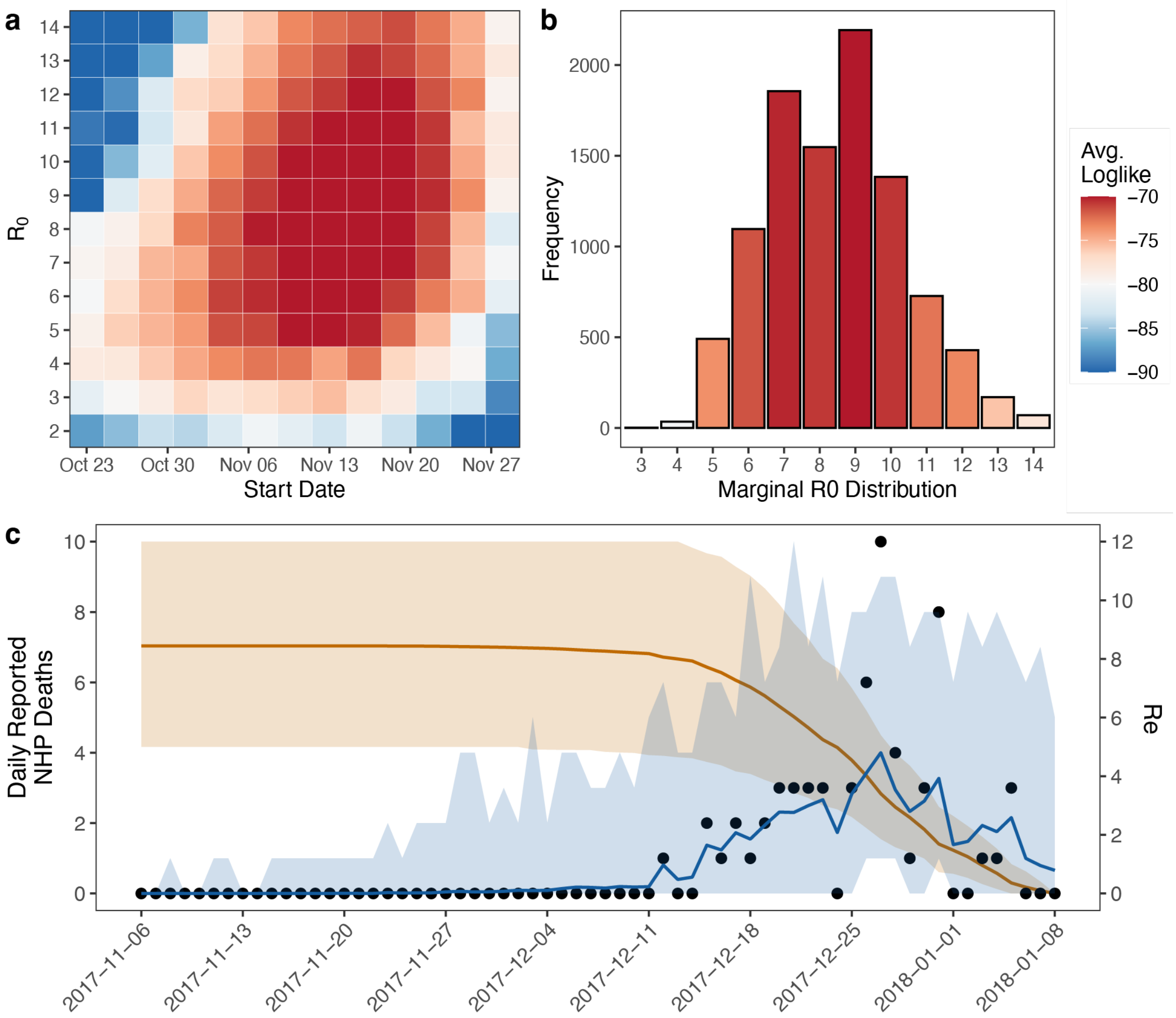

Supplementary Fig. 12. Estimate of the reproduction number and transmission dynamics in PEAL assuming a later timing of importation based on the MRCA of Cluster A. a. Average log-likelihood (colour scale) for each joint combination of the basic reproduction number (R_0, y-axis) and outbreak start date (x-axis). Warmer tones indicate parameter pairs with higher posterior support. **b.** Marginal posterior distribution of R_0 integrating over all start-date hypotheses shown in panel a. Bar height denotes posterior sample frequency; colours match the log-likelihood scale used in panel a. **c.** Model fit to daily reported nonhuman-primate (NHP) deaths (black circles, left axis) and the corresponding effective reproduction number over time (R_e, orange line, right axis). Blue line and shaded ribbon give the posterior median and 95% credible interval for model-predicted deaths; the orange ribbon shows the 95% credible interval for R_e.

Supplementary Table 1. Univariate negative-binomial models of *Hg. leucocelaenus* abundance and individual lagged meteorological variables. Columns show separate models in which the monthly mosquito catch is related to a single meteorological variable (temperature, humidity or cumulative rainfall) recorded one month before trapping. Significance levels: *P<0.1, **P<0.05, ***P<0.01. Coefficients are given with standard errors in parentheses; wihle pseudo-R^2, log-likelihood, over-dispersion parameter (θ) and AIC are shown below.

	Dependent variable: Mosquitoes captured													
	(1)	(2)	(3)	(4)	(5)	(6)	(7)	(8)	(9)	(10)	(11)	(12)	(13)	(14)
cum_rain	0.918***							-0.174	-0.162	-0.227	0.081			
	(0.351)							(0.653)	(0.424)	(0.445)	(0.434)			
min_temp		1.835***								2.117***				
		(0.313)								(0.585)				
mean_temp			1.928***					2.140***	2.134***			1.871***	1.995***	1.778***
			(0.323)					(0.628)	(0.586)			(0.412)	(0.393)	(0.327)
max_temp				2.050***							1.943***			
				(0.393)							(0.656)			
min_hum					1.564**			0.016					-0.136	
					(0.615)			(0.698)					(0.454)	
mean_hum						2.466***						0.143		
						(0.781)						(0.663)		
max_hum							1.694**							0.645
							(0.713)							(0.421)
Constant	2.880***	2.324***	2.495***	2.737***	2.777***	1.962***	2.444***	2.499***	2.503***	2.305***	2.719***	2.428***	2.532***	2.063***
	(0.379)	(0.282)	(0.265)	(0.277)	(0.477)	(0.563)	(0.600)	(0.310)	(0.269)	(0.283)	(0.291)	(0.406)	(0.294)	(0.365)
pseudo-R2	0.485	0.827	0.833	0.772	0.306	0.441	0.242	0.837	0.837	0.835	0.774	0.834	0.835	0.873
Observations	8	8	8	8	8	8	8	8	8	8	8	8	8	8
Log Likelihood	-34.316	-30.004	-29.878	-31.023	-35.629	-34.664	-36.029	-29.779	-29.779	-29.835	-30.997	-29.854	-29.825	-28.909
theta	1.015** (0.497)	2.675* (1.468)	2.764* (1.525)	2.125* (1.153)	0.756** (0.344)	0.924** (0.436)	0.696** (0.312)	2.796* (1.531)	2.799* (1.533)	2.734* (1.482)	2.143* (1.166)	2.786* (1.541)	2.802* (1.550)	3.491* (1.967)
Akaike Inf. Crit.	72.632	64.009	63.755	66.046	75.258	73.327	76.057	67.558	65.559	65.669	67.994	65.709	65.650	63.818

Note: *p<0.1;**p<0.05;***p<0.01

Supplementary Table 2. Multivariate negative-binomial models of *Hg. leucocelaenus* abundance and meteorological variables. Each column reports a separate model specification in which monthly mosquito counts are regressed on different combinations, transformations (quadratic, logarithmic) and interactions of temperature and rainfall measured in the same month as *Hg. leucocelanus* collections. Model statistics and significance levels are as in **Supplementary Table 4**.

	Dependent variable: Mosquitoes captured											
	(1)	(2)	(3)	(4)	(5)	(6)	(7)	(8)	(9)	(10)	(11)	(12)
mean_temp	0.932***						6.236			0.900**		
	(0.256)						(4.277)			(0.454)		
min_temp		0.822***						3.708			0.707*	
		(0.227)						(2.375)			(0.373)	
max_temp			0.903***						7.897			1.067*
			(0.305)						(6.642)			(0.621)
I(mean_temp2)							-0.137					
							(0.107)					
I(min_temp2)								-0.091				
								(0.071)				
I(max_temp2)									-0.146			
									(0.135)			
cum_rain	-2.094	-2.930	1.042				-29.700**	-34.063***	-25.341*	-6.626	-17.506	25.933
	(5.472)	(5.737)	(5.601)				(12.286)	(11.946)	(13.708)	(53.821)	(38.975)	(82.664)
log(mean_temp)				19.342***								
				(4.412)								
log(min_temp)					14.410***							
					(3.288)							
log(max_temp)						23.824***						
						(6.707)						
log(cum_rain)				-0.324	-0.447	-0.019						
				(0.501)	(0.524)	(0.537)						
I(cum_rain2)							112.285**	123.731***	104.309**			
							(45.356)	(42.944)	(49.574)			
mean_temp:cum_rain										0.221		
										(2.620)		
min_temp:cum_rain											0.829	
											(2.212)	
max_temp:cum_rain												-1.004
												(3.346)
Constant	-15.596***	-10.628***	-19.485***	-55.842***	-38.790***	-73.431***	-65.559	-32.092	-102.168	-14.949*	-8.735	-23.455
	(4.578)	(3.243)	(6.937)	(14.136)	(10.256)	(22.400)	(42.554)	(19.699)	(81.756)	(8.663)	(5.835)	(14.757)
pseudo-R2	0.837	0.835	0.774	0.849	0.851	0.777	0.912	0.921	0.861	0.838	0.838	0.776
Observations	8	8	8	8	8	8	8	8	8	8	8	8
Log Likelihood	-29.779	-29.835	-30.997	-29.515	-29.472	-30.950	-27.658	-27.308	-29.247	-29.776	-29.764	-30.951
theta	2.799* (1.533)	2.734* (1.482)	2.143* (1.166)	2.971* (1.637)	2.962* (1.616)	2.156* (1.171)	5.609 (3.755)	6.467 (4.527)	3.751 (2.440)	2.813* (1.546)	2.821* (1.549)	2.138* (1.153)
Akaike Inf. Crit.	65.559	65.669	67.994	65.030	64.944	67.900	65.316	64.615	68.494	67.551	67.528	69.903

Note: *p<0.1; **p<0.05; ***p<0.01

Supplementary Table 3. Statistics for the sequences generated in this study obtained through metagenomics. Dash (–)=not available. Ct=Cycle threshold. Groups I–III are described in **Supplementary Fig. S1**. Days PM = days post-mortem. Ct=RT-qPCR cycle threshold. No.=number; bp=base pairs. Ref. (%)=Percentage YFV reference covered.

Accession Number	Group	Days PM	PEAL Zone	Ct	Total Reads	Mapped Reads	No. bp >10x	Ref. (%)
OQ714247.1	I	–	B	21	818114	3472	8275	76.2
OQ714248.1	I	–	B	24	265510	5744	10439	96.1
OQ714249.1	I	–	B	23	422256	5705	10846	99.9
OQ714241.1	I	–	B	23	451634	9862	10589	97.5
OQ714242.1	I	–	B	24	345856	1100	10247	94.4
OQ714243.1	I	–	B	25	250509	2776	10845	99.9
OQ714244.1	I	–	B	19	306772	2017	10459	96.3
OQ714245.1	I	–	B	23	446908	12624	10848	99.9
OQ714246.1	I	–	C	22	1164917	4784	10736	98.9
OQ714250.1	II	3–5	A	–	367336	23288	10849	99.9
OQ714284.1	II	0–2	A	9	56402	14362	10849	99.9
OQ714314.1	II	0–2	A	17	82781	798	10660	98.2
OQ714285.1	II	3–5	A	17	106855	10762	10849	99.9
OQ714292.1	II	3–5	A	–	203729	6566	10848	99.9
OQ714317.1	II	3–5	A	–	774456	10175	10848	99.9
OQ714318.1	II	0–2	A	18	213953	7039	10848	99.9
OQ714320.1	II	3–5	A	–	447068	4574	10687	98.4
OQ714321.1	II	3–5	A	–	247208	29285	10848	99.9
OQ714326.1	II	0–2	A	19	182932	2106	10846	99.9
OQ714327.1	II	0–2	A	19	182920	11361	10848	99.9
OQ714271.1	II	0–2	B	11	407008	48210	10849	99.9
OQ714303.1	II	0–2	B	17	113347	34444	10849	99.9
OQ714274.1	II	0–2	B	9	230812	89420	10849	99.9
OQ714307.1	II	0–2	B	15	477906	50804	10849	99.9
OQ714280.1	II	0–2	B	11	51104	11179	10849	99.9
OQ714309.1	II	0–2	B	20	513994	3969	10848	99.9
OQ714310.1	II	0–2	B	17	258941	1042	10687	98.4
OQ714283.1	II	0–2	B	11	281965	29986	10849	99.9
ON022359.1	II	0–2	B	7	25325	8259	10849	99.9
OQ714312.1	II	0–2	B	–	321847	27924	10848	99.9
OQ714315.1	II	3–5	B	19	72960	2592	10848	99.9
OQ714319.1	II	0–2	B	18	340900	1474	10845	99.9
OQ714277.1	II	0–2	C	11	95800	13739	10847	99.9
OQ714272.1	II	0–2	C	10	440140	211290	10849	99.9

OQ714304.1	II	0–2	C	20	228897	4823	10848	99.9
OQ714305.1	II	0–2	C	27	333557	15745	10847	99.9
OQ714306.1	II	0–2	C	18	247967	2887	10848	99.9
OQ714282.1	II	0–2	C	9	82830	24694	10849	99.9
OQ714313.1	II	0–2	C	–	469318	1386	7876	72.5
OQ714316.1	II	0–2	C	18	278911	15073	10849	99.9
OQ714311.1	II	3–5	C	–	74426	4450	10846	99.9
OQ714252.1	III	0–2	–	7	136409	48114	10850	99.9
OQ714294.1	III	–	–	18	480266	13427	10849	99.9
OQ714295.1	III	–	–	18	165616	5098	10554	97.2
OQ714251.1	III	–	–	9	347015	120679	10847	99.9
OQ714253.1	III	–	–	10	251799	34505	10849	99.9
OQ714254.1	III	–	–	11	454728	82792	10847	99.9
OQ714296.1	III	–	–	21	441411	16200	10849	99.9
OQ714297.1	III	–	–	18	392374	18459	10848	99.9
OQ714298.1	III	–	–	21	302079	8108	10849	99.9
OQ714255.1	III	–	–	10	239597	47888	10849	99.9
OQ714275.1	III	–	–	–	484365	7601	10846	99.9
OQ714299.1	III	–	–	18	91287	509	10415	95.9
OQ714273.1	III	–	–	11	484434	88869	10849	99.9
OQ714300.1	III	–	–	19	166039	4917	9702	89.3
OQ714301.1	III	–	–	23	105262	32858	10847	99.9
OQ714269.1	III	–	–	14	522481	68992	10847	99.9
OQ714278.1	III	–	–	10	330242	75341	10847	99.9
OQ714268.1	III	–	–	13	511264	39921	10849	99.9
OQ714276.1	III	–	–	11	101153	11952	10847	99.9
OQ714279.1	III	0–2	–	8	309212	29184	10849	99.9
OQ714266.1	III	–	–	14	94539	17626	10849	99.9
OQ714267.1	III	–	–	10	373188	162990	10849	99.9
OQ714265.1	III	0–2	–	8	75263	13808	10849	99.9
OQ714264.1	III	–	–	11	257570	39011	10847	99.9
OQ714270.1	III	–	–	9	48873	5942	10847	99.9
OQ714256.1	III	–	–	7	69433	24286	10848	99.9
OQ714257.1	III	0–2	–	7	33774	13820	10847	99.9
OQ714258.1	III	0–2	–	6	90213	36640	10850	99.9
OQ714261.1	III	–	–	12	268706	33408	10849	99.9
OQ714262.1	III	–	–	10	302435	70310	10849	99.9
OQ714259.1	III	–	–	7	93556	7100	10847	99.9
OQ714260.1	III	–	–	13	393533	40746	10849	99.9
OQ714263.1	III	–	–	9	253456	92692	10849	99.9
OQ714302.1	III	–	–	19	171720	3774	10815	99.6

OQ714281.1	III	–	–	11	64560	13694	10847	99.9
OQ714308.1	III	–	–	18	285030	2251	10848	99.9
OQ714289.1	III	–	–	14	107070	7361	10847	99.9
OQ714288.1	III	3–5	–	10	601563	89604	10849	99.9
OQ714287.1	III	–	–	15	156755	2879	10635	97.9
OQ714286.1	III	0–2	–	13	165251	21016	10849	99.9
OQ714290.1	III	–	–	12	113202	10084	10849	99.9
OQ714322.1	III	–	–	–	40114	3293	10848	99.9
OQ714323.1	III	3–5	–	18	54729	1342	9261	85.3
OQ714324.1	III	–	–	21	253266	10740	10848	99.9
OQ714325.1	III	–	–	17	500519	30204	10849	99.9
OQ714293.1	III	0–2	–	12	170149	7447	10847	99.9
OQ714328.1	III	–	–	15	281528	70286	10849	99.9

Supplementary Table 4. Description of the IBM model parameterisation and sources for model parameters.

Parameter	Description	Reference
Transmission Rate (β)	Transmission rate parameter. Inferred directly from PEAL time-series data using particle filter-based likelihood estimation approach.	NA
Incubation period duration	Gamma distribution with shape X and rate Y giving average duration of Z days. Delay distribution exposed to infectious (i.e. the incubation period for YFV) in *A. guariba*. Estimated from analysis of data from Haemmert et al, 1950 (see **Fig. 4c–e**). Inverse of the expectation of this distribution is γ used in the calculation of R_0	Laemmert et al, 1950[12]
Duration of infectiousness	Gamma distribution with shape X and rate Y giving average duration of Z days. Delay between *Alouatta* becoming infectious and dying from YFV. Estimated from analysis of data from Haemmert et al, 1950 (see Fig. S8).	Laemmert et al, 1950[12]
EIP	Gamma distribution with shape X and rate Y giving average duration of Z days. Extrinsic incubation period i.e. the time taken for infected *Haemagogus* mosquitoes to become infectious. Estimated from analysis of data from Bates & Roca-Gacia, 1946 (see **Fig. 4c–e**). Gamma distribution with shape X and rate Y.	Bates & Roca-Garcia, 1946[13]
Delay between death and observation	Exponential distribution rate parameter X. The delay between *A. guariba* death occurring, and that death being detected, reported and enumerated. This was estimated empirically from veterinarian estimated stage of corpse decomposition at detection (i.e. the number of days since the NP had died).	Empirically estimated
p_{obs}	0.7625 (61 / 80) Probability of a dead *A. guariba* belonging to the PEAL population being detected, reported and successfully enumerated during the outbreak. Estimated empirically as the fraction of enumerated deaths relative to the overall known size of the *A. guariba* population in PEAL at the outbreak's start.	Empirically estimated

References

1. Abreu, F. V. S. D. *et al. Haemagogus leucocelaenus* and *Haemagogus janthinomys* are the primary vectors in the major yellow fever outbreak in Brazil, 2016–2018. *Emerging Microbes & Infections* **8**, 218–231 (2019).
2. Stanzani, L. M. D. A. *et al.* Back to Where It Was First Described: Vectors of Sylvatic Yellow Fever Transmission in the 2017 Outbreak in Espírito Santo, Brazil. *Viruses* **14**, 2805 (2022).
3. Vasconcelos, P. F. C. *et al.* An Epidemic of Sylvatic Yellow Fever in the Southeast Region of Maranhao State, Brazil, 1993–1994: Epidemiologic and Entomologic Findings. *The American Journal of Tropical Medicine and Hygiene* **57**, 132–137 (1997).
4. Caleiro, G. S. *et al.* Yellow Fever Virus (YFV) Detection in Different Species of Culicids Collected During an Outbreak in Southeastern Brazil, 2016–2019. *TropicalMed* **10**, 118 (2025).
5. De Oliveira, C. H. *et al.* Yellow Fever Virus Maintained by Sabethes Mosquitoes during the Dry Season in Cerrado, a Semiarid Region of Brazil, in 2021. *Viruses* **15**, 757 (2023).
6. Hill, S. C. *et al. Climate and Land-Use Shape the Spread of Zoonotic Yellow Fever Virus*. http://medrxiv.org/lookup/doi/10.1101/2022.08.25.22278983 (2022) doi:10.1101/2022.08.25.22278983.
7. Bryant, J. E., Holmes, E. C. & Barrett, A. D. T. Out of Africa: A Molecular Perspective on the Introduction of Yellow Fever Virus into the Americas. *PLoS Pathog* **3**, e75 (2007).
8. Gómez, M. M. *et al.* Genomic and structural features of the yellow fever virus from the 2016–2017 Brazilian outbreak. *Journal of General Virology* **99**, 536–548 (2018).
9. Delatorre, E. *et al.* Distinct YFV Lineages Co-circulated in the Central-Western and Southeastern Brazilian Regions From 2015 to 2018. *Front. Microbiol.* **10**, 1079 (2019).
10. Mir, D. *et al.* Phylodynamics of Yellow Fever Virus in the Americas: new insights into the origin of the 2017 Brazilian outbreak. *Sci Rep* **7**, 7385 (2017).
11. Faria, N. R. *et al.* Genomic and epidemiological monitoring of yellow fever virus transmission potential. *Science* **361**, 894–899 (2018).
12. Laemmert, H. W. & Kumm, H. W. The Susceptibility of Howler Monkeys to Yellow Fever Virus. *The American Journal of Tropical Medicine* **s1-30**, 723–731 (1950).
13. Roca-García, M. & Bates, M. The Development of the Virus of Yellow Fever in Haemagogus Mosquitoes 1. *The American Journal of Tropical Medicine and Hygiene* **s1-26**, 585–605 (1946).